JACS
JOURNAL OF THE AMERICAN CHEMICAL SOCIETY

Article

pubs.acs.org/JACS

Supramolecularly Engineered Perylene Bisimide Assemblies Exhibiting Thermal Transition from Columnar to Multilamellar Structures

Shiki Yagai,*[,†,‡] Mari Usui,[†] Tomohiro Seki,[†] Haruno Murayama,[§] Yoshihiro Kikkawa,[⊥] Shinobu Uemura,[¶] Takashi Karatsu,[†] Akihide Kitamura,[†] Atsushi Asano,[#] and Shu Seki[#]

[†]Department of Applied Chemistry & Biochemistry, Graduate School of Engineering, Chiba University, 1-33 Yayoi-cho, Inage-ku, Chiba 263-8522, Japan

[‡]CREST, Japan Science and Technology Agency (JST), 1-33 Yayoi-cho, Inage-ku, Chiba 263-8522, Japan

[§]Office of Society-Academia Collaboration for Innovation, Kyoto University, Yoshida-Honmachi, Sakyo-ku, Kyoto 606-8501, Japan

[⊥]National Institute of Advanced Industrial Science and Technology (AIST), 1-1-1 Higashi, Tsukuba, Ibaraki 305-8562, Japan

[¶]Department of Applied Chemistry & Biochemistry, Graduate School of Science and Technology, Kumamoto University, Kurokami 2-39-1, Kumamoto 860-8555, Japan

[#]Department of Applied Chemistry, Graduate School of Engineering, Osaka University, 2-1, Yamadaoka, Suita, Osaka 565-0871, Japan

Supporting Information

ABSTRACT: Perylene 3,4:9,10-tetracarboxylic acid bisimide (PBI) was functionalized with ditopic cyanuric acid to organize it into complex columnar architectures through the formation of hydrogen-bonded supermacrocycles (rosette) by complexing with ditopic melamines possessing solubilizing alkoxyphenyl substituents. The aggregation study in solution using UV−vis and NMR spectroscopies showed the formation of extended aggregates through hydrogen-bonding and $\pi-\pi$ stacking interactions. The cylindrical fibrillar nanostructures were visualized by microscopic techniques (AFM, TEM), and the formation of lyotropic mesophase was confirmed by polarized optical microscopy and SEM. X-ray diffraction study revealed that a well-defined hexagonal columnar (Col_h) structure was formed by solution-casting of fibrillar assemblies. All of these results are consistent with the formation of hydrogen-bonded PBI rosettes that spontaneously organize into the Col_h structure. Upon heating the Col_h structure in the bulk state, a structural transition to a highly ordered lamellar (Lam) structure was observed by variable-temperature X-ray diffraction, differential scanning calorimetry, and AFM studies. IR study showed that the rearrangement of the hydrogen-bonding motifs occurs during the structural transition. These results suggest that such a striking structural transition is aided by the reorganization in the lowest level of self-organization, i.e., the rearrangement of hydrogen-bonded motifs from rosette to linear tape. A remarkable increase in the transient photoconductivity was observed by the flash-photolysis time-resolved microwave conductivity (FP-TRMC) measurements upon converting the Col_h structure to the Lam structure. Transient absorption spectroscopy revealed that electron transfer from electron-donating alkoxyphenyl groups of melamine components to electron-deficient PBI moieties takes place, resulting in a higher probability of charge carrier generation in the Lam structure compared to the Col_h structure.

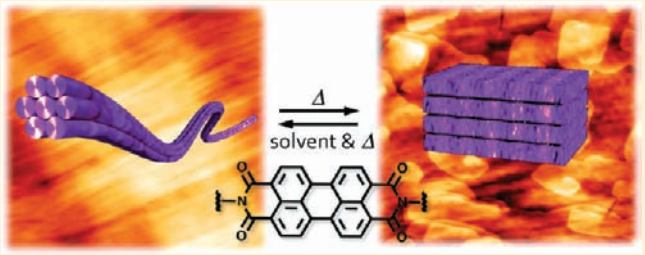

INTRODUCTION

Supramolecularly engineered functional dye assemblies and related π-systems offer unique features such as size- and dimension-controlled nanoarchitectures, novel optical and electronic properties, stimuli-responsive properties, and remarkably versatile material properties that are inaccessible via the conventional aggregation of dyes.[1] These unique features open a new avenue for supramolecular chemists to invent practical, cutting-edge organic materials that are applicable especially in the field of organic electronics and photonics.

Perylene 3,4:9,10-tetracarboxylic acid bisimide (PBI) dyes,[2] which are potentially useful colorants, are among the most intensively studied functional dyes based on supramolecular approaches.[1a,2a,3] n-Type semiconductivity[4] and fruitful optical properties,[5] combined with ease of chemical functionalization,[6] make PBI dyes well-suited building blocks not only for the fabrication of supramolecular electronic materials but also for the evaluation of the rationality of applied supramolecular

Received: March 16, 2012
Published: April 19, 2012

   dx.doi.org/10.1021/ja302574b | J. Am. Chem. Soc. 2012, 134, 7983−7994

approaches in both structural and functional aspects. Pioneered by Würthner et al.,[7] the introduction of wedge-shaped substituents[8] into the imide positions of PBIs has been employed as a promising strategy to construct one-dimensional columnar assemblies with remarkable functional features such as supramolecular chirality,[9] liquid crystallinity,[10] and intracolumnar charge transportation.[10a,11] The introduction of swallow tail substituents also affords columnar liquid crystalline materials[12] and enables the fabrication of phase-separated nanofibers.[13] Because the self-assembly of these discotic PBIs are mainly driven by $\pi-\pi$ stacking interactions, only oligomeric stacks are formed in solution, and only in the bulk state do they form extended columnar assemblies reaching nanometer size regime.[10a] The formation of well-defined columnar assemblies in the solution phase is potentially useful for the development of nanostructured electronic devices. The use of polymer scaffolds is one of the promising strategies to obtain well-defined columnar arrays of PBIs.[14]

The incorporation of additional noncovalent interactions also could render PBI stacks' well-defined columnar assemblies stable in solution. For examples, the introduction of amide or urea hydrogen-bonding networks in the parallel direction to the $\pi-\pi$ stacking axis enables the formation of elongated fibrous assemblies that form organogels.[15] In contrast, the application of more directional interactions, such as multiple hydrogen bonds,[16] in the orthogonal direction to the stacking axis furnishes dye assemblies with more hierarchically organized superstructures[17,18] and also realizes a supramolecular p−n heterojunction between the separated stacks of donors and acceptors.[18a,b]

Among diverse hydrogen-bonded supramolecular scaffolds that can be used for the bottom-up construction of multicomponent supramolecular self-assemblies,[10e,16g−j] cyclic hexamer so-called rosettes formed by three ditopic melamine (M) units and cyanurate (CA) or barbiturate (BA) units are among the most well-studied discrete supramolecular systems. M·CA and M·BA rosettes have been intensively studied by the groups of Whitesides[16a,19] and Reinhoudt[16c,20] with the concept of covalent preorganization and cooperativity in multicomponent supramolecular assemblies, respectively. Experimental[21] and theoretical[22] investigations focusing on the competing formation of extended tapelike (linear or crinkled) hydrogen-bonded motif have been carried out. Beyond the frameworks of archetypal examples for discrete supramolecular systems, some rosettes have been designed to assemble into extended columnar architectures.[23] However, the construction of well-defined columnar assemblies decorated with functional π-systems using M·CA rosettes has been scarcely explored[24] while several one-component rosettes have yielded functional columnar π-nanostructures.[25] Furthermore, if one can control the hydrogen-bonded motifs of M·CA complexes by changing the complementary component or external stimuli,[26] different types of self-assembled π-nanoarchitectures could be obtained though the hierarchical organization. This approach thus enables the investigation of the structure−function relationship in the self-organized π-systems with a minimum of structural modification for the molecular components.

Here we report the supramolecular assemblies consisting of CA-functionalized PBI dye (CAPBI) and complementary melamines possessing aliphatic chains (Figure 1). Various spectroscopic and microscopic investigations suggested that these complementary components construct well-defined columnar assemblies in organic solvents through the formation

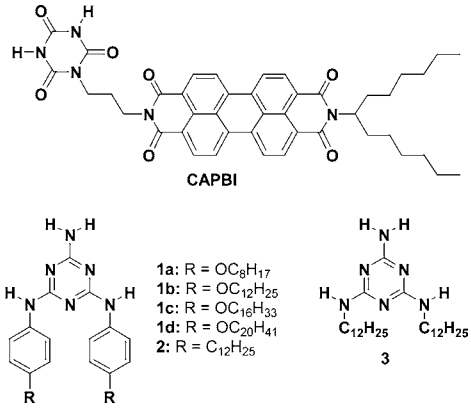

Figure 1. Structures of CA-functionalized PBI (CAPBI) and melamines **1a−d**, **2**, and **3**.

of hydrogen-bonded rosettes. Upon casting the solutions, these columnar assemblies further organized into hexagonal columnar structures as revealed by X-ray diffraction experiments. The formation of columnar structures depended on the solubilizing substituents in the melamine modules that influence the solubilities of competing tapelike assemblies. Interestingly, a dramatic structural change from columnar to lamellar architectures was observed for the assemblies upon applying thermal stimuli in the bulk state (Scheme 1). The resulting lamellar structure can be reconverted to the original columnar one by redissolution in organic solvent and subsequent solution-casting. Such a well-defined transition in self-assembled architectures of functional π-systems upon applying external stimuli is a very attractive property as a stimuli-responsive material because it may induce a large change in optoelectronic properties. We thus investigated optoelectronic properties of CAPBI·**1b** assemblies by flash-photolysis time-resolved microwave conductivity (FP-TRMC) and transient absorption spectroscopy experiments and revealed a remarkable change in photoinduced charge separation efficiency between PBI chromophores and alkoxyphenyl groups of **1b** upon the structural transition.

RESULTS AND DISCUSSION

Synthesis. CAPBI was synthesized by the reaction of (3-aminopropyl)cyanurate with *N*-swallow-tailed perylene monoimide monoanhydride. As complementary components, we prepared ditopic melamines **1a−d**, which differ in the length of their alkyl chains. The alkoxyphenyl groups serve to greatly increase solubilities of their supramolecular assemblies with CAPBI. For comparison we also employed melamine **3**[17b] whose dodecyl chains are introduced directly into the melamine module. Melamine **2** possessing dodecylphenyl groups was also prepared for exploring the possibility of electron transfer from electron-donating alkoxyphenyl groups of **1** to electron-accepting PBI moieties in the assemblies.

NMR and UV−vis Studies. CAPBI is poorly soluble in chloroform. However, once it was dissolved in 1,1,2,2-tetrachloroethane in the presence of 1 equiv of **1b** and then the solvent was evaporated, the homogeneous solids were obtained, which are soluble in chloroform at millimolar concentrations. When CAPBI was mixed with **1b** in excess, precipitation took place (Figure S1, Supporting Information).

^{1}H NMR spectra of the 1:1 molar mixture of CAPBI and **1b** in $CDCl_3$ at the concentrations of both components ranging

dx.doi.org/10.1021/ja302574b | J. Am. Chem. Soc. 2012, 134, 7983−7994

Scheme 1. Thermoresponsive Supramolecular Organization of CAPBI·1b[a]

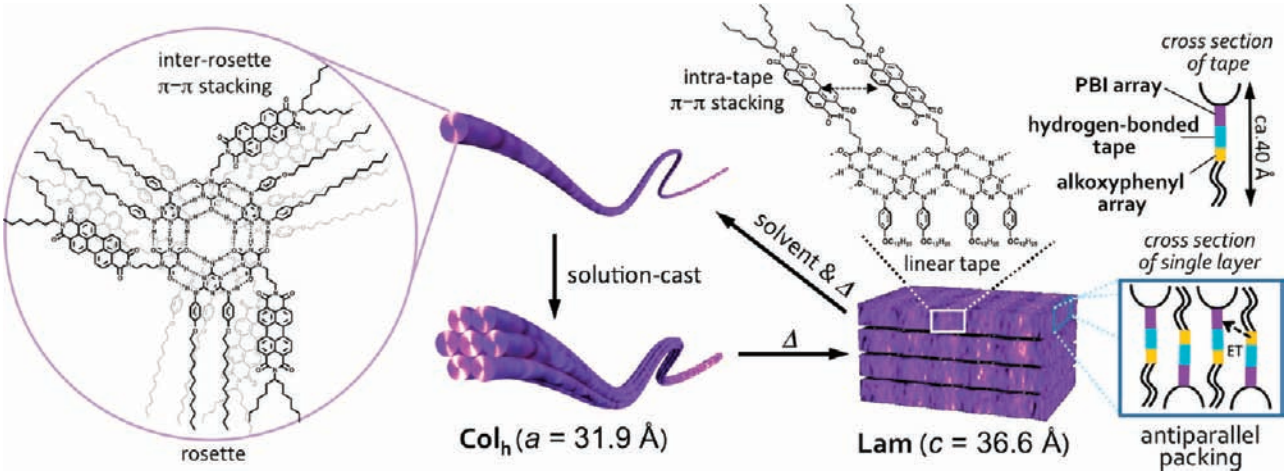

[a]For the Lam structure, antiparallel packing arrangement of linear tapes can be proposed from X-ray diffraction and transient absorption spectroscopic studies.

from 1.0×10^{-3} to 5.0×10^{-3} M showed markedly broadened resonance (Figure 2a), indicating the formation of high

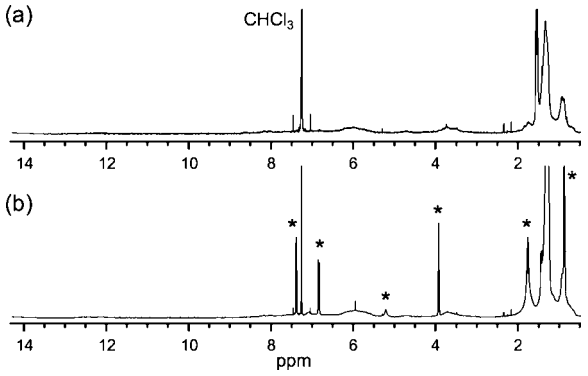

Figure 2. ^{1}H NMR spectra of (a) 1:1 and (b) 1:1.5 molar mixtures of CAPBI (c = 5.0×10^{-3} M) and **1b** (c = 5.0×10^{-3} M or 7.5×10^{-3} M) in $CDCl_3$ at 25 °C. The sharp resonances denoted by asterisk in b derive from free **1b**.

molecular-weight assemblies. No appreciable spectral change was observed upon heating the 1.0×10^{-3} M solution to 60 °C, illustrating a remarkably high stability of our PBI assemblies compared to those formed purely by $\pi-\pi$ stacking interactions[10a,27] and even by hydrogen-bond-assisted $\pi-\pi$ stacking interactions.[15b,28] When a mixture was prepared with excess **1b** (1.5 equiv), sharp resonances of free **1b** were observed in addition to the broadened resonances of the assemblies (Figure 2b). For this mixture, a nearly 1:0.5 molar ratio between aggregated and free **1b** was confirmed by integration of the corresponding resonances, thus confirming the formation of stable 1:1 assemblies (hereafter will be referred to as CAPBI·**1b**).

The UV–vis spectra of chloroform solutions of CAPBI·**1b** were recorded upon changing the concentration from 1.0×10^{-2} M to 5.0×10^{-6} M (Figure 3a). At high concentrations, less structured spectra typical of $\pi-\pi$ stacked PBI aggregates were observed.[10a,12c,15c,27,29] The spectra were almost unchanged when the concentration was above 5.0×10^{-3} M. Upon dilution, a transition to a structured spectrum with λ_{max} at 527, 490, and 459 nm was observed, suggesting the dissociation

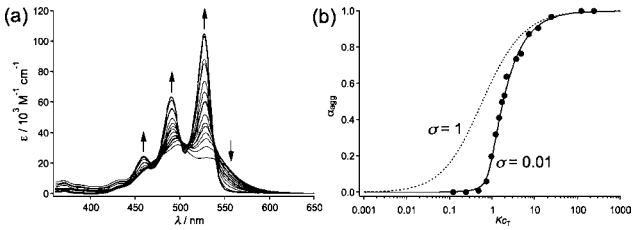

Figure 3. (a) Concentration-dependent UV–vis spectra of the 1:1 molar mixture of CAPBI and **1b** in chloroform ([CAPBI] = [**1b**] = 1.0×10^{-6} to 5.0×10^{-3} M). Arrows indicate the spectral changes with decreasing concentration. (b) Solid and dashed curves: fractions of aggregated molecules α_{agg} plotted as a function of Kc_T with the nucleation factor σ of 1 (dotted curve, isodesmic model) and 0.01 (solid curve, K_2–K nucleation–growth model). For details, see ref 35. Closed circles: plot of experimental α_{agg} calculated from the UV–vis data of spectra (a) versus Kc_T. c_T is the total concentrations of the components ([CAPBI] + [**1b**]).

of the assemblies. Below 1.0×10^{-5} M, the spectral transition leveled off. From the obtained concentration-dependent data, we calculated fractions of aggregated molecule α_{agg} for every recorded concentration and plotted them as a function of the total concentration of the components (c_T = [CAPBI] + [**1b**]). Nonlinear least-squares regression analysis of the plot with the isodesmic model[30] resulted in failure (see dotted curve in Figure 3b), suggesting the involvement of a cooperative mechanism consisting of the formation of hydrogen-bonded assemblies and their hierarchical organization driven by $\pi-\pi$ stacking interactions. We thus employed a nucleation–elongation model[31] that has been applied to synthetic assemblies.[32] Recently, the simplest version of this model (the K_2–K model) has been applied to the concentration-dependent NMR[33] and UV–vis[34] data obtained from supramolecular polymerization of PBI derivatives. In this model, one dimerization process from monomeric species is assumed to be nucleation dominated by equilibrium constant K_2 (or K_{nuc}), which is followed by isodesmic elongation steps ($K_3 = K_4 ... = K_i ... = K$). In the present system, the nucleation process might involve the formation of various types of multicomponent hydrogen-bonded assemblies. However, based on the following microscopic and X-ray diffraction studies, it is evident that the

dx.doi.org/10.1021/ja302574b | J. Am. Chem. Soc. 2012, 134, 7983–7994

nucleation in the present system progresses toward the formation of only one type of multicomponent assembly (i.e., rosette), which further stacks to form one-dimensional columnar structures. We thus assumed that the apparent equilibrium constant K_{app} as K_2 for the formation of such an assembly from other competing open-ended assemblies as well as monomeric species.[22] As shown in Figure 3b, the calculated curve (α_{agg} vs Kc_T) showed the best fit to the experimental plot when the nucleation factor σ (= K_{app}/K) was set to 0.01 and isodesmic equilibrium constant K to 12000 M^{-1}, thus giving a K_{app} value of 120 M^{-1}. The significantly small K_{app} compared to the K value indicates that the nucleation involves the formation of multicomponent assemblies held together by triple hydrogen-bonding interactions between melamine and cyanurate (K_{dim} = 300−5000 M^{-1} in chloroform).[22] On the other hand, the large K value in chloroform (permittivity ε = 4.81) is remarkable because most aggregation studies for monochromophoric PBI derivatives have been performed using nonpolar solvents such as methylcyclohexane (ε = 2.24), giving isodesmic equilibrium constants on the order of 10^4 M^{-1}.[35] This implies that the elongation step in the present system is driven by multipoint $\pi-\pi$ stacking interactions of multichromophoric hydrogen-bonded assemblies.[17b,24e]

TEM and AFM Studies. To obtain fully $\pi-\pi$ stacked assemblies in dilute solutions, we investigated CAPBI·**1b** in methylcyclohexane (MCH). Although CAPBI is hardly soluble in MCH, its 1:1 molar mixture with **1b** is highly soluble in this nonpolar solvent. In contrast to the concentration-dependent UV−vis spectra observed in chloroform, MCH solutions of the assemblies showed a spectrum typical of fully $\pi-\pi$ stacked PBIs (λ_{max} = 497 nm) even upon decreasing the concentration to c = 1.0 × 10^{-5} M (Figure S2, Supporting Information). Furthermore, no temperature dependence was observed for this dilute solution upon heating to 90 °C, suggesting the formation of fairly stable $\pi-\pi$ stacked assemblies.

Nanostructures of CAPBI·**1b** were studied by transmission electron microscope (TEM) and atomic force microscope (AFM). TEM images of the assemblies formed in a dilute MCH solution (c = 1.0 × 10^{-4} M) displayed entangled networks of fibrous structures with widths of 10−50 nm (Figure 4a,b). Thinner fibrils of widths less that 10 nm were often observed (arrow in Figure 4b). AFM observation of the assemblies spin-coated on highly oriented pyrolytic graphite (HOPG) visualized the hierarchical organization of the elementary fibrils into higher-order bundled structures (Figure 4c,d). The cross-sectional analysis of the bundled parts revealed that fibrils have a uniform height of 2.9 nm (Figure S3, Supporting Information). The observed uniformity in the elementary nanostructures as well as their side-by-side packing strongly suggests that CAPBI·**1b** forms a rigid cylindrical columnar nanostructure.

Lyotropic Liquid Crystals and Mesoscopic Structures. When sufficiently long cylindrical aggregates are formed and their anisotropic organization takes place in solution, lyotropic liquid crystals (LCs) might be formed.[36] Increasing the concentration of MCH solutions of CAPBI·**1b** to millimolar regime led to the formation of translucent viscous solutions (Figure 5a). The viscous solutions were stable and did not form precipitates upon storage for over 1 year. Upon drying the viscous solutions, mesoscopic fibrous superstructures were observed by scanning electron microscopy (Figure 5b). The widths of fibers are in the range of 100−1000 nm, indicating

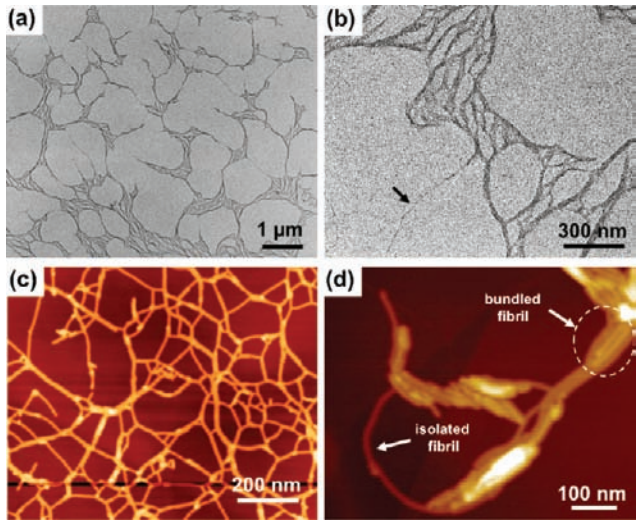

Figure 4. (a, b) TEM and (c, d) AFM height image (z scale: 20 nm) of CAPBI·**1b**. The samples were prepared by spin-coating the assemblies (c = 1.0 × 10^{-4} M) in MCH onto carbon-coated copper grids (for TEM) or HOPG (for AFM). TEM samples were stained with uranyl acetate.

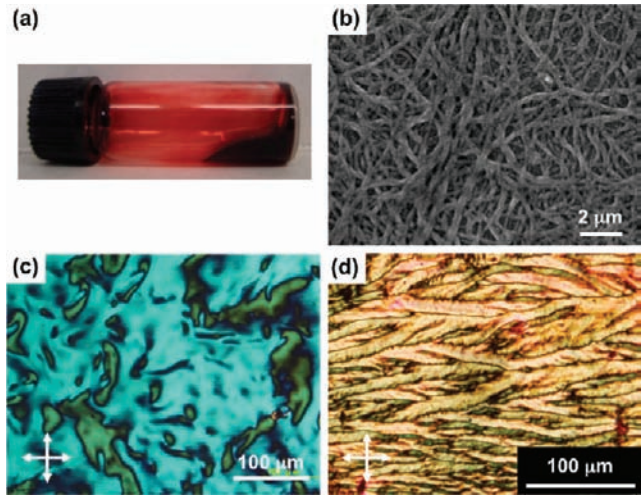

Figure 5. (a) Photograph of a lyotropic LC of CAPBI·**1b** in MCH (5.2 wt %, c = 5.0 × 10^{-3} M) taken just after laying the vial. (b) SEM image of a dried lyotropic LC. (c) POM image of a lyotropic LC sandwitched between two glass slides. (d) POM image of a lyotropic LC dried between two glass slides.

the hierarchical organization of hundreds of elementary fibrils into the mesoscopic superstructures.

Observation by polarized optical microscopy (POM) of the viscous solutions sandwiched between two glass slides showed a pronounced birefringence (Figure 5c), indicating the formation of a lyotropic LC due to the anisotropic organization of the fibrillar nanostructures. Lyotropic LCs could also be obtained with *n*-alkanes, toluene, and even chloroform at high concentrations (c > 5.0 × 10^{-2} M). When these lyotropic LCs were sandwiched between two glass slides and the solvent was slowly evaporated, strongly birefringent textures as shown in Figure 5d were observed. Such striated textures have been observed for cylindrical J-aggregates of pseudoisocyanine,[37] supramolecular polymers of merocyanine H-aggregates,[38] and other hydrogen-bonded supramolecular polymers[39] and have

been explained by undulation of cylindrical fibers due to their thermomechanical instability.[37]

Packing Structure of Fibrils. Powder X-ray diffraction (XRD) measurements of lyotropic LCs of CAPBI·**1b** using various solvents all showed a single broad diffraction, which might correspond to the average center-to-center distance of fibrils in the bundles. For only concentrated lyotropic LCs of dodecane (>50 wt %), intense diffractions at around 31.5 Å were followed by small diffractions at 14.3 and 11.3 Å, suggesting the presence of a 2-D ordering of fibrils (Figure S4, Supporting Information). For all the lyotropic LCs, however, thin films obtained by evaporation of solvent displayed the almost identical XRD patterns composed of diffraction peaks at d = 27.1, 15.8, 13.5, and 10.2 Å (see blue diffractogram in Figure 9a). These diffractions are unequivocally assignable to (100), (110), (200), and (210) diffractions, respectively, from a hexagonal columnar (Col_h) ordering with the lattice constant a = 31.9 Å. The formation of Col_h structures by solution processing without any thermal treatment is notable, demonstrating the formation of well-defined cylindrical fibrils.

The above fibrils could be macroscopically oriented by mechanical shearing of lyotropic LCs between two glass substrates until it became an apparently solvent-free state. The resulting thin films showed maximum birefringence when the shearing direction was oriented 45° to the direction of the polarizers (Figure 6a,b). Using a 530-nm (first-order red) retardation plate, negative birefringence of the fibrils (the refractive index of the fibrils is higher along their short axis) was revealed (Figure 6c,d). This observation is consistent with the columnar aggregates of *N,N′*-di(3,4,5-tridodecyloxyphenyl) PBI,[18e] suggesting a relatively perpendicular orientation of perylene π-plane with respect to the long axis of the fibrils. A

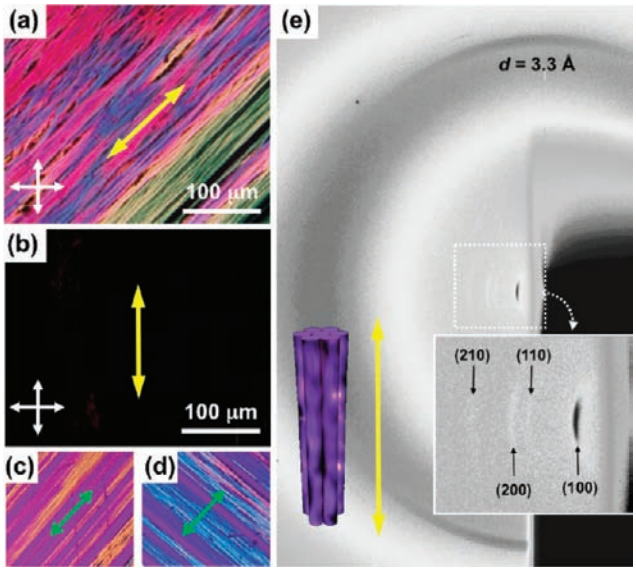

Figure 6. (a,b) Polarized optical micrographs of a sheared film of CAPBI·**1b** oriented (a) 45° to a polarizer and (b) parallel to polarizers. Yellow arrows indicate the shearing direction. The white arrows indicate the directions of polarizer and analyzer. (c, d) Polarized optical micrographs of the same sheared film oriented (c) parallel and (d) perpendicular to the slow axis of a 530-nm retardation plate (green arrows). (e) WAXD (SPring-8, BL02B2, λ = 0.8 Å) of a sheared film of the assemblies CAPBI·**1b**. Inset shows the orientation of the hexagonal columnar structures with respect to the diffractogram. The yellow arrow indicates the shearing direction.

trasmission-mode 2D wide-angle X-ray diffraction (WAXD) of a sheared films on a ultrathin glass substrate (thickness = 0.03 mm) with synchrotron radiation exhibited a diffraction corresponding to d-spacing of 3.3 Å in the meridional direction,[10c] whereas diffractions corresponding to the Col_h ordering appeared in the equatorial direction (Figure 6e). The former diffraction corresponds to the $\pi-\pi$ stacking distance of PBI stacks running along the columnar axis.[40]

Thermal Transition from Columnar to Lamellar Structures. DSC, POM and XRD Studies. We found that the solubility of thoroughly dried Col_h films of CAPBI·**1b** remarkably decreases by thermal treatment. When the thin films prepared on glass substrate were immersed in chloroform before and after thermal annealing at 200 °C for 5 min, the former was completely dissolved whereas the latter was peeled off from the substrate without dissolution (Figure 7). Vigorous

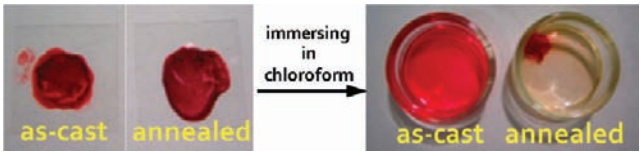

Figure 7. Immersion test of a thin film of CAPBI·**1b** prepared on a cover glass in chloroform before and after annealing at 200 °C for 5 min.

heating of the peeled film in chloroform for a few hours with ultrasonication afforded a homogeneous solution, which upon casting restored the Col_h structure as confirmed by XRD analysis. Although the increase of crystallinity by thermal annealing is commonly observed for crystalline compounds, a dramatic change in the self-assembled structures was indicated for our assemblies by following experiments.

A differential scanning calorimetry (DSC) thermogram of CAPBI·**1b** recorded with a scan rate of 5 °C/min is shown in Figure 8. The first heating scan disclosed the presence of a

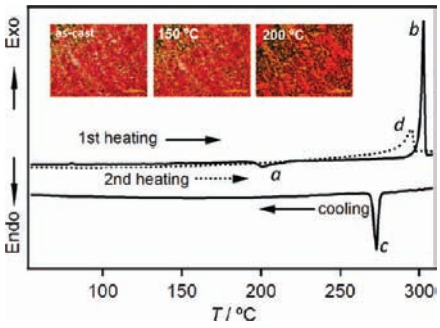

Figure 8. DSC chart of CAPBI·**1b**. Scan rate: 5 °C/min. The sample was prepared by drying the MCH solution of the assembly. Insets show the POM images at r.t., 150 °C, and 200 °C.

broad exothermic transition at 200 °C (peak a, ΔH = 13.6 kJ/mol), indicating the occurrence of a thermally induced structural ordering. Upon further heating, an endothermic melting transition was observed at 302 °C (peak b, ΔH = 71.3 kJ/mol). Upon cooling the isotropic melt, only an exothermic peak was observed at 273 °C (peak c, ΔH = 40.6 kJ/mol) which indicates the crystallization. The second heating scan did not show the above exothermic transition, and only the melting transition was observed at 295 °C (peak d, ΔH = 33.8 kJ/mol).

dx.doi.org/10.1021/ja302574b | J. Am. Chem. Soc. 2012, 134, 7983−7994

The observation by POM with mechanical stress revealed that the solid sample of CAPBI·**1b** becomes soft at around 150 °C but retains strong birefringence in the first heating treatment (inset in Figure 8), suggesting the formation of a soft crystalline phase undetectable by DSC. Upon further heating to 200 °C where DSC showed the exothermic transition, however, the sample again became stiff. This observation further supports the occurrence of a certain structural ordering at 200 °C. In line with the DSC study, these changes were not observed in the cooling process of the isotropic melt and the subsequent second heating treatment of the "annealed" material, suggesting that the thermal transitions are irreversible processes. A careful observation of the sample by POM led us to conclude that CAPBI·**1b** does not form a thermotropic liquid crystalline mesophase.

Interestingly, the variable-temperature XRD experiment of the Col_h film of CAPBI·**1b** revealed that the exothermic transition observed in the first heating scan of DSC is accompanied by a large structural change from the Col_h to a lamellar (Lam) structure via the formation of an intermediate phase. Figure 9a and 9b shows the change of XRD patterns of CAPBI·**1b** upon heating to 200 °C and the subsequent cooling. From 25 °C to 125 °C, the thermal reorganization of the Col_h structure occurred as shown by the increase of the diffraction intensities. Above 130 °C, the diffractions started to diminish, and at 150 °C, diffractions could not be observed at all. Further heating to 175–200 °C resulted in the emergence of a sharp diffraction at d = 36.6 Å which was followed by small diffractions with a spacing ratio of 1/2, 1/3, 1/5, and 1/6, suggesting the formation of an ordered multilamellar structure with the interlayer spacing of 36.6 Å. In Figure 9c, the relative diffraction intensities of the (100) diffraction (intercolumnar distance) of the Col_h structure and the (001) diffraction (interlayer distance) of the Lam structure are plotted versus temperature. The plots illustrate that the Col_h and the Lam structures do not exist complimentary to each other, and they both disappear at 150 °C (indicated by arrow). It should be noted that the same structural transition with the identical transition temperature occurs irrespective of the solvent employed for the preparation of the films. *Hence, it can be concluded that the Col_h → Lam transition is not caused by the evaporation of solvents entrapped in the assemblies and an intrinsic property of the assemblies in the bulk state.*

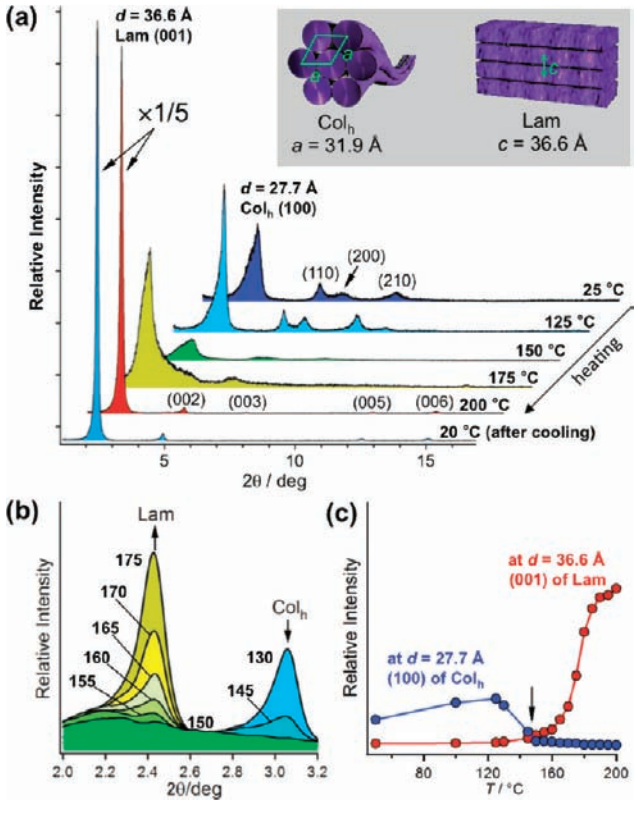

Figure 9. Variable temperature XRD experiments of a film of CAPBI·**1b**. (a) Change of XRD patterns (2θ = 1.1–17°, Cu Kα) upon heating (25–200 °C, 5.0 min for every scan) and subsequent cooling to 20 °C. Inset shows the schematic representation of the Col_h and the Lam structures with their lattice parameters. (b) XRD patterns around the transition temperature. (c) Temperature-dependence of the relative diffraction intensities at d = 27.7 (for the Col_h structure) and 36.6 Å (for the Lam structure).

To exclude the possibility of a thermal disassembly of CAPBI·**1b** to form Lam structures consisting of either of the individual components, we also carried out variable-temperature XRD experiments of the individual components, CAPBI and **1b** (Figure S5, Supporting Information). CAPBI did not show explicit diffraction peaks at r.t. Upon heating to 220 °C, a structural ordering occurred, exhibiting diffractions assignable to a lamellar structure with a layer spacing of 43.9 Å. The layer spacing does not match that of the Lam structure of CAPBI·**1b**. On the other hand, **1b** already showed a clear diffraction at d = 36.5 Å at room temperature. Upon heating, a fluidal mesophase appeared at 150 °C, exhibiting higher-order diffractions assignable to a lamellar structure with a layer spacing of 37.9 Å (smectic liquid crystal). Although this layer spacing of **1b** is close to that of the Lam phase of CAPBI·**1b** (d = 36.6 Å), **1b** entered the isotropic phase at 175 °C, which is lower over 100 °C than that of CAPBI·**1b** (302 °C). Furthermore, the diffraction peaks of **1b** are discernible only up to (003) under the same experimental condition, highlighting that a long-range ordered Lam structure is constructed by CAPBI·**1b**.

Thermal Transition from Columnar to Lamellar Structures. AFM, IR, and UV–vis Studies. The thermal Col_h → Lam transition of CAPBI·**1b** was studied by AFM. Figure 10 shows the change of the surface morphology of the Col_h film by thermal treatment (annealing) at different temperatures. For the as-cast film, ribbonlike nanostructures[41] with a smooth surface could be imaged, and the individual fibrils (columns) as observed for the diluted assemblies were not observed (Figure 10a). Upon annealing the film at 100 °C for 1 min, rather straight rodlike nanostructures were imaged everywhere together with the ribbonlike structures (Figure 10b), which is consistent with increased hexagonal ordering of columns as also shown by the XRD study. Upon increasing the annealing temperature to 150 °C, these ribbons and rods melted to form a wide-range smooth surface (Figure 10c). Because no X-ray diffraction was observed at around this temperature (Figure 9b) but the film remained birefringent (Figure 8), it is most likely that the individual columns were dispersed from Col_h bundles by melting of aliphatic tails, a situation which resembles that of nematic columnar mesophases. Interestingly, further increase of the annealing temper-

dx.doi.org/10.1021/ja302574b | J. Am. Chem. Soc. 2012, 134, 7983–7994

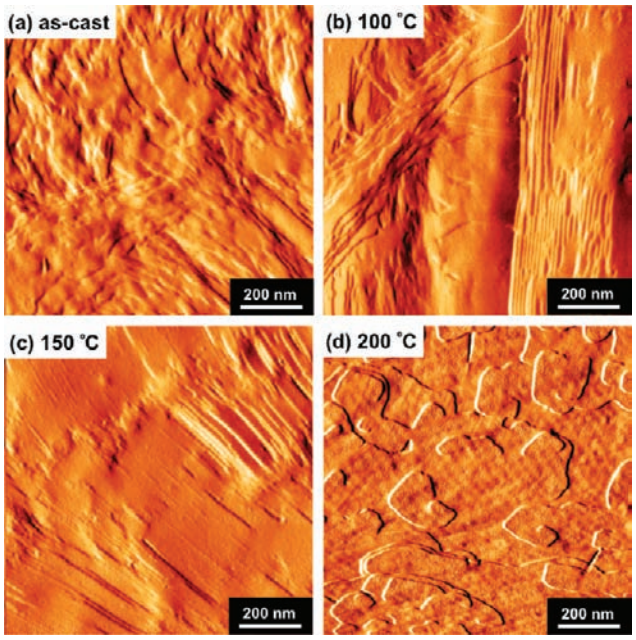

Figure 10. AFM amplitude images of a film of CAPBI·**1b** (a) without and (b–d) with annealing at different temperatures. (a) As-cast film. (b–d) Annealed at (b) 100 °C, (c) 150 °C, and (d) 200 °C.

ature to 200 °C led to the evolution of terraced nanostructures (Figure 10d). The average thickness of terraces is 3.5 ± 0.47 nm, which is in good agreement with the interlayer distance of the Lam structure. This AFM experiment clearly shows that the Col_h → Lam transition is accompanied by a drastic structural change of the nanoscopic self-assembled structures.

The variable-temperature IR measurement confirmed the rearrangement of hydrogen-bonding motif upon the Col_h → Lam transition. Solvent-free films of CAPBI·**1b** displayed three N–H stretching vibrations at 3400 (band A), 3300 (band B), and 3221 cm^{-1} (band C) arising from the primary and the secondary amino groups of **1b** and the cyanurate moiety of CAPBI (Figure 11a). Upon an increase in temperature, a decrease in the intensity of band C was observed as an overall spectral change. To clarify the correlation between such a

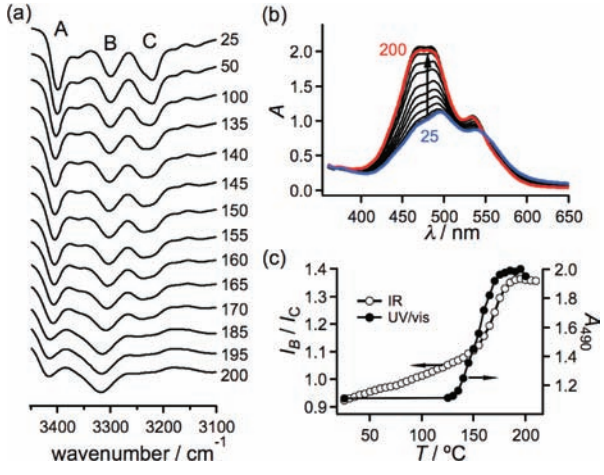

Figure 11. Variable-temperature (a) IR and (b) reflection spectra of thin films of CAPBI·**1b** (25 → 200 °C). (c) Plots of the intensity ratio of bands B and C (I_B/I_C, left axis) in part a and the absorbance at 490 nm (A_{490}, right axis) in part b versus temperature.

spectral change and temperature, we plotted the intensity ratio of band B and band C (I_B/I_C) versus temperature (Figure 11c, left axis). Below 150 °C, a gradual increase of I_B/I_C was observed upon increasing temperature. This moderate change might be due to the structural reorganization of the hydrogen-bonding motif in the Col_h structure. Above 150 °C where the Lam structure is emerging, however, a steep increase of I_B/I_C was observed, and the spectrum recorded at 200 °C apparently features two bands at 3400 and 3284 cm^{-1}. This change is ascribable to the shift of band C to a higher frequency region (ca. 3360 cm^{-1}) to coalesce with band B. This spectrum is not consistent with summations of the spectra of the two separate compounds after annealing (Figure S6, Supporting Information). These results unequivocally demonstrate that the Col_h → Lam transition is accompanied by the rearrangement of M·CA hydrogen-bonding motifs between melamine and cyanurate modules.

Variable-temperature reflection spectroscopy of CAPBI·**1b** further revealed that the π–π stacking arrangement of PBI moieties undergoes a substantial change upon the Col_h → Lam transition (Figure 11b,c). Below 130 °C, the film showed the spectra similar to those observed for solution-phase PBI stacks with rotational displacements.[10a,42] Such rotational displacements generally induce the formation of columnar π–π-stacked structures.[7,10a,12e,43] Above 130 °C, the absorption band in 400–500 nm gradually increased and the shoulder around 530 nm became more structured. The spectrum recorded at 200 °C is very similar to that of PBI derivatives possessing long linear aliphatic tails that are organized in lamellar structures.[12c,29b]

Effect of Substituents. Because solubilities of M·CA and M·BA assemblies are an important parameter to determine supramolecular structures (rosettes or tapes) in the solid state,[22,26,44] we investigated CAPBI·**1a**, CAPBI·**1c**, CAPBI·**1d**, CAPBI·**2**, and CAPBI·**3**. The solid samples of these assemblies were prepared by evaporating homogeneous 1,1,2,2-tetrachloroethane solutions of the 1:1 molar mixtures. As detailed in Supporting Information, CAPBI·**1c**, CAPBI·**1d**, and CAPBI·**2** showed good solubilities in organic solvents. For these assemblies, XRD (Figure S7, Supporting Information) and AFM (Figures S8–11, Supporting Information) revealed the occurrence of organization behaviors similar to that of CAPBI·**1b**. On the other hand, CAPBI·**1a** and CAPBI·**3** showed poor solubilities, and different organization behaviors were revealed by XRD and AFM studies.

Proposed Organization Models of CAPBI·Melamine Assemblies into Col_h Structures. The solution-state NMR and UV–vis studies revealed that CAPBI and **1b** coassemble to form soluble and polymeric assemblies by a nucleation–elongation mechanism that has not been observed for PBI assemblies formed mainly by π–π stacking interactions. The XRD studies under ambient conditions demonstrated that soluble assemblies formed by CAPBI·**1b–1d** and CAPBI·**2** could organize into defined Col_h structures via solution-casting (Figure S7). The formation of two-dimensionally ordered columnar structures from soluble, noncrystalline PBI assemblies without any annealing treatment is remarkable, illustrating that well-defined cylindrical columnar assemblies are already formed in solution. This was further supported by the fibrillar nanostructures visualized by AFM as well as the formation of lyotropic liquid crystals (Figure 4c; Figures S9–S11). Combining these insights, it can be proposed that these soluble assemblies form rosettes which further stack to form cylindrical columnar nanostructures (Scheme 1).[23b,e,25a,45]

dx.doi.org/10.1021/ja302574b | J. Am. Chem. Soc. 2012, 134, 7983–7994

In contrast, insoluble assemblies CAPBI·**1a** and CAPBI·**3** did not form Col_h structures but displayed a complex XRD pattern (CAPBI·**1a**) or no well-defined peaks (CAPBI·**3**), suggesting that these systems do not form rosettes as major assemblies. The study of M·CA and M·BA hydrogen-bonded assemblies has been pioneered by Whitesides and co-workers since the early 1990s.[16a,46] The accumulation of single crystal X-ray structures of diverse assemblies with different substituents was enough to conclude that the assemblies with melamines possessing bulky substituents result in the rosette architecture rather than extended (linear or crinkled) tapelike architectures. This finding was explained in terms of repulsive steric interactions between the melamine components in tapelike assemblies in the dynamic solution state (the concept of peripheral crowding).[19a,21,47] Because our assemblies all feature linear alkyl chains, the steric factor cannot explain the observed relationship between the solubilities and the organization behaviors.

In 2001, Reinhoudt and co-workers reported a theoretical reevaluation of this concept and concluded that the bulkiness of the substituents has a small impact on the fraction of rosettes versus competing oligomeric tapelike assemblies in the solution phase if the solubilities of tapelike assemblies are high comparably to that of rosettes.[22] In such a situation, rosettes are dominant species in the solution and obtained as crystals or precipitates upon evaporation. However, if the solubilities of competing tapelike assemblies are significantly low compared to that of rosette due to the absence of bulky substituents that could decrease their planarity, such open-ended assemblies are crystallized even though they are minor components in the solution phase. This mechanism is in line with our results. Octyloxyphenyl groups of **1a** and dodecyl groups of **3** are believed not to endow their oligomeric tapelike assemblies with solubilities enough to hold the equilibrium with rosettes. Accordingly, complex mixtures of various tapes with different lengths would precipitate upon evaporating the 1,1,2,2-tetrachloroethane solutions.

While the formation of cylindrical columnar nanostructures in the solution phase and their hexagonal packing in the bulk state are strong evidence of the formation of rosettes for the soluble assemblies, the detailed packing structure of rosettes within columns is not clear in the present study. Figure S14, Supporting Information, shows a force-field-optimized molecular model of CAPBI·**1b** rosette. Although perylene π-planes in this model are tilted against the hydrogen-bonded plane, they may take an optimized conformation upon stacking into columns. The longest width of the rosette in projection is 52 Å, which is rather longer than the lattice constant a (31.9 Å) of the Col_h structure of CAPBI·**1b**. This difference might be due to considerable void space within the rosette, allowing the interdigitation of exterior alkyl chains. However, based on the lattice constant a = 31.9 Å and the $\pi-\pi$ stacking distance of PBIs (3.3 Å) observed in the WAXD study, the number of CAPBI+**1b** pairs per lattice (Z value) falls to 1.5 assuming the density of 1.0 g cm^{-3}. Therefore, the lattice based on the $\pi-\pi$ stacking distance of PBIs is too small to accommodate one rosette (Z = 3). This discrepancy in the Z values indicates that the $\pi-\pi$ stacking distance of PBIs does not correspond to the lattice parameter c (thickness of the disk) of the Col_h structure. The lattice parameter c in the present system might be rather long due to the deviation of the rosette core from planarity. Reinhoudt et al. reported an intracolumnar periodicity of 8.4 Å for liquid crystalline double rosette assemblies.[23d]

Proposed Mechanism of Thermal Transition from Col_h to Lam Structures. The thermally induced structural transition from Col_h to Lam structures observed for the solvent-free solids of the soluble assemblies is unusual behavior for the organization of functional π-systems decorated with aliphatic chains, because usually lamellar to columnar transition is induced at high temperatures by microsegregation between rigid molecular segments and sterically demanding molten alkyl chains.[48] For M·CA and M·BA hydrogen-bonded assemblies, the linear tapelike hydrogen-bonded motif[17a,49] is geometrically the most conformable hydrogen-bonded scaffold to hierarchically organize crystalline multilamellar structures.[44,50] Molecular modeling of the hexadecameric linear tape of CAPBI·**1b** shows intratape $\pi-\pi$ staking interactions between PBI chromophores (Figure S15, Supporting Information; Scheme 1). Such a "closed" π-surface within tapes may allow their antiparallel packing to form a single layer, which compensates for their noncentrosymmetric architecture that is inconsonant with the observed high crystallinity of the Lam structure (Scheme 1). This packing fashion could explain the interlayer spacing of 36.6 Å observed for the Lam structure of CAPBI·**1b**, which matches very well with the width of the molecular modeled tape (ca. 40 Å, Figure S15).

Taking into account the results of the AFM (Figure 10) and the IR studies (Figure 11a), we thus proposed that the rearrangement of the hydrogen-bonded motif from rosette to linear tape is responsible for this unique thermally induced structural transition. The effect of a tiny amount of residual solvents whose evaporation could cause the precipitation of tapes can be excluded by the observation of the solvent-dependence for the Col_h → Lam transition temperatures. Guanosine[51] and folic acid derivatives[16k,50c,d,52] have been known to form ribbonlike and disclike hydrogen-bonded motifs depending on the substituents and the experimental conditions. However, no thermal structural transition was observed between the two motifs although metal cations enable dynamic conversion of ribbonlike to disclike motifs in the mesomorphic state.

The solution-phase hierarchical organization of CAPBI·melamine rosettes into columnar nanostructures is a result of subtle matching of rather strong multipoint $\pi-\pi$ stacking interactions on peripheral PBI moieties and relatively loose stacking of the hydrogen-bonded rosette core. Such kinetically formed nanostructures could be retained upon removal of solvents at ambient conditions. However, as shown by variable- temperature reflection spectroscopy (Figure 11b), thermal treatment triggered a rearrangement of the PBI stacks into the energetically more favorable crystalline packing.[53] Such crystalline PBI stacks might be structurally incompatible with loosely stacked rosettes due to mismatch in their packing efficiencies, and the system may release the accumulated strain energy by rearranging the hydrogen-bonded motif to more crystalline linear tapes in the mobile soft crystalline phase.

Optoelectronic Properties. The optoelectronic properties of CAPBI·**1b** in the bulk state were studied by flash-photolysis time-resolved microwave conductivity (FP-TRMC) measurements, informative for the short-range transient conductivities of materials.[10d,29b,54] Upon excitation of the Col_h film of CAPBI·**1b** with a laser pulse at 355 nm, a pronounced transient conductivity, given by $\phi\sum\mu$ (ϕ, photocarrier generation yield; $\sum\mu$, sum of the mobilities of photogenerated charge carriers) was observed (Figure 12a). The maximum transient conductivity was estimated to be 1.9×10^{-4} cm^2 V^{-1} s^{-1} from the

dx.doi.org/10.1021/ja302574b | J. Am. Chem. Soc. 2012, 134, 7983−7994

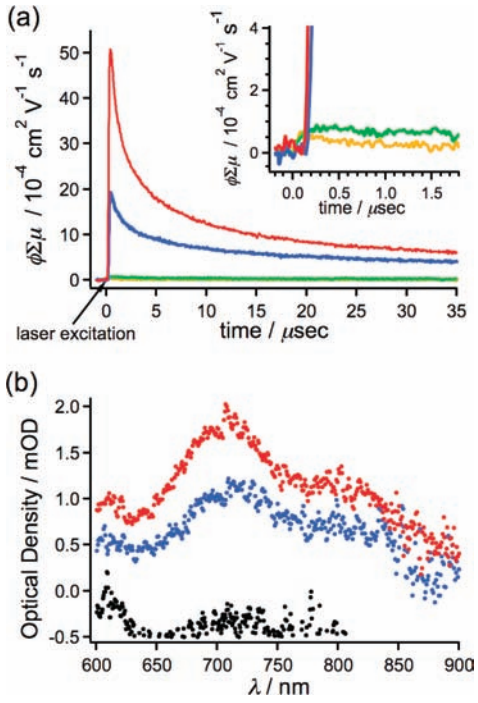

Figure 12. (a) Conductivity transients of thin films of CAPBI (green), **1b** (orange), and CAPBI·**1b** in the Col_h structure (blue) and in the Lam structure (red) observed upon excitation with a 355 nm laser pulse (photon density =1.4 × 10^{16} photons cm^{-2}). Inset is a magnification of the graph around the laser excitation. (b) Transient absorption spectra of CAPBI·**1b** in the Col_h structure (blue) and in the Lam structure (red) and of CAPBI·**2** in the Lam structure (black) observed after 2 μs upon excitation with a 355 nm laser pulse (photon density = 1.8 × 10^{16} photons cm^{-2}).

end-of-pulse conductivity. Because negligible TRMC signals were observed for the films of the individual components CAPBI and **1b** (green and orange curves in Figure 12a, respectively), the remarkable TRMC signal indicates the occurrence of efficient charge carrier generation upon photoexcitation and subsequent charge carrier transportation in the assemblies. For a sheared thin film as shown in Figure 6a, we set the film in a microwave cavity, in such a way that the shearing direction was parallel or perpendicular to the standing electric field direction of the microwave cavity, and recorded TRMC signals. Approximately 2-fold greater transient conductivity was observed along the shearing direction ($\phi\sum\mu\parallel$ = 3.0 × 10^{-6} cm^2 V^{-1} s^{-1}, $\phi\sum\mu\perp$ = 1.5 × 10^{-6} cm^2 V^{-1} s^{-1}), demonstrating that the charge carriers are more mobile along the long axis of the fibrils.

A prominent increase of transient conductivity was observed when the Col_h film was annealed at 200 °C for several minutes to form the Lam structure (Figure 12a). The $\phi\sum\mu$ values increased to 5.0 × 10^{-4} cm^2 V^{-1} s^{-1}, which is 2.6-fold greater than that of the Col_h structure. This observation indicates that the Lam structure has a higher quantum yield of photocarrier generation (ϕ) and/or higher mobility of the resulting charge carriers ($\sum\mu$) compared to the Col_h structure. To clarify this point, we measured ϕ by transient absorption spectroscopy. Upon exposure of the Col_h and the Lam films to laser pulses at 355 nm, a prominent transient absorption band characteristic of PBI radical anions (PBI^{-}) was observed at 720 nm (Figure 12b).[55] Because the observed radical anion species has a lifetime of at least 2 μs, the decomposition of the donor moieties might take place to give a long-lived PBI radical anion due to the absence of charge recombination.[56] An extinction coefficient of PBI radical anions had been reported to be 7.4 × 10^4 cm^{-1} mol^{-1} dm^3 (at 712 nm) per charge,[55b] which allowed estimation of the concentration of the photogenerated negative charges (PBI^{-}) from the kinetic traces at 720 nm. The values of ϕ for the Col_h and the Lam structures were estimated to be 0.93 × 10^{-3} and 2.0 × 10^{-3}, respectively, immediately after pulse exposure (Table 1).

Table 1. Transient Conductivities ($\phi\sum\mu$) Determined by Flash-Photolysis Time-Resolved Microwave Conductivity (FP-TRMC), Quantum Yields of the Photocarrier Generation (ϕ determined by transient absorption spectroscopy), and Sum of the Mobility of Charge Carriers ($\sum\mu$) for the Col_h Structures (before annealing) and Lam Structures (after annealing) of CAPBI·1b and CAPBI·2

assemblies	structure	$\phi\sum\mu^a$	ϕ	$\sum\mu^a$
CAPBI·**1b**	Col_h	1.9 × 10^{-4}	0.93 × 10^{-3}	0.20
	Lam	5.0 × 10^{-4}	2.0 × 10^{-3}	0.25
CAPBI·**2**	Col_h	2.9 × 10^{-6}	–	–
	Lam	7.7 × 10^{-5}	–	–

[a] In cm^2 V^{-1} s^{-1}.

With the values of ϕ and $\phi\sum\mu$, the sum of the mobility of charge carriers ($\sum\mu$) was calculated to be 0.20 cm^2 V^{-1} s^{-1} for the Col_h structure, and 0.25 cm^2 V^{-1} s^{-1} for the Lam structure of CAPBI·**1b**. The mobility value of the Col_h structure is higher than those of room-temperature columnar LCs of *N*,*N*′-bis(3,4,5-tridodecyloxyphenyl)-PBI (0.0078 cm^2 V^{-1} s^{-1}) and *N*,*N*′-bis(3,4,5-tridodecyloxybenzyl)-PBI (0.011 cm^2 V^{-1} s^{-1}),[10d] and that of *N*,*N*′-bis(3,4,5-tridodecylphenyl)-PBI in the crystalline (0.14 cm^2 V^{-1} s^{-1}) or columnar LC state (0.0076 cm^2 V^{-1} s^{-1}),[10a] all measured by pulse-radiolysis time-resolved microwave conductivity (PR-TRMC). Furthermore, the mobility of the Lam structure is comparable to those of *N*,*N*′-dioctadecyl-PBI in the polycrystalline state (0.2 cm^2 V^{-1} s^{-1}).[29b] These finding indicates that our assemblies form PBI stacks with potentially high mobilities of charge carriers. More importantly, our TRMC experiments revealed that the Col_h → Lam structural transition facilitates the charge separation (ϕ, 2.2-fold) more pronouncedly than the mobility of the charge carriers ($\sum\mu$, 1.3-fold).

Wasielewski[18a,56] and Würthner et al.[7,57] reported that alkoxyphenyl groups serve as an electron-donor to electron-deficient PBI chromophores. Wasielewski et al. further reported electron transfer from triethylamine to PBI derivatives.[56a] Both situations could occur in the present systems where solubilizing alkoxyphenyl substituents or amino groups of the melamine modules can serve as electron-donating moieties. Indeed, no fluorescence emission from PBI chromophores was observed for CAPBI·**1b** even in the diluted solution state. To clarify the electron transfer pathways in our assemblies, we investigated optical properties of CAPBI·**2** that show almost the same supramolecular organization process as that of CAPBI·**1b**, but it involves less electron-donating alkylphenyl substituents.[10a] Thin films of CAPBI·**2** exhibited excimer-like fluorescence of PBI chromophores at 619 nm (Figure S16, Supporting Information). Furthermore, transient absorption spectroscopy showed negligibly weak absorption of PBI^{-} (Figure 12b). These results lead us to conclude that the electron transfer in the present assemblies occurs from the alkoxyphenyl

dx.doi.org/10.1021/ja302574b | J. Am. Chem. Soc. 2012, 134, 7983−7994

substituents of **1b** to the perylene chromophore of CAPBI, in these cases giving 1 (in the Lam structures) or 2 orders of magnitude (in the Col_h structures) lower FP-TRMC signals in CAPBI·**2** than in CAPBI·**1b** (Table 1).

The above insight offers a reasonable explanation for the observed increase of photocarrier generation upon the $Col_h \rightarrow$ Lam transition. As already described in a previous section, the antiparallel stacking of linear tapes of CAPBI·**1b** within a single layer is the most feasible secondary structure to compensate for their noncentrosymmetric structures (Scheme 1). This assumption is strongly supported by the interlayer spacing of 36.6 Å, which is nearly consistent with the width of a molecular modeled linear tape (ca. 40 Å, Figure S15). This stacking fashion enables the close proximity of electron-deficient perylene moieties of CAPBI to the electron-rich alkoxyphenyl moieties of **1b** compared to stacked rosettes.

CONCLUSION

In this study, we have shown that well-defined columnar assembly of PBI dyes can be constructed by melamine·cyanurate hydrogen-bond supramolecular systems. The formation of lyotropic mesophases in nonpolar solvents and well-defined hexagonal columnar lattices in solution-cast films of the 1:1 mixtures of CAPBI and melamines with long aliphatic substituents suggests that hydrogen-bonded rosettes possessing three PBI chromophores are formed in solution, and they are hierarchically organized into cylindrical columnar assemblies. Such columnar assemblies could be visualized by TEM and AFM as well-defined fibrillar nanostructures. The solubility of the assemblies and the formation of well-defined Col_h structures depend strongly on the substituents of the melamine modules, consistent with a previously proposed mechanism for the selection of rosette/tape structures in the solid state.[22] Another outstanding property of our PBI assemblies is the thermal convertibility of the Col_h structures to the Lam structures in the bulk state as revealed by the XRD study. IR, AFM, and UV/vis studies demonstrated that such a striking structural transition occurs through the rearrangement of the hydrogen-bonded motifs from rosettes to linear tapes and was suggested to be caused by the mismatch in the packing efficiency between the stacks of hydrogen-bonded rosette cores and the thermodynamically stable crystalline stacks of PBIs. Furthermore, a remarkable change in the optoelectronic properties was revealed for the $Col_h \rightarrow$ Lam transition by FP-TRMC and transient absorption studies as a result of the dislocation of the donor and the acceptor chromophores. The present study thus represents a new aspect of supramolecular dye assemblies as a strategy to obtain stimuli-responsive functional material[58] by integrating biologically related dynamic supramolecular systems and artificial functional π-systems.

ASSOCIATED CONTENT

Supporting Information

Synthesis and characterization data of CAPBI and melamine **1a–d**, **2**, and **3**, detailed description of spectroscopic/microscopic studies and device fabrication, additional UV–vis, AFM, XRD, and IR data. This material is available free of charge via the Internet at http://pubs.acs.org.

AUTHOR INFORMATION

Corresponding Author

yagai@faculty.chiba-u.jp

Notes

The authors declare no competing financial interest.

ACKNOWLEDGMENTS

S.Y. thanks Izumi Science and Technology Foundation and The Sumitomo Foundation for partial financial support.

REFERENCES

(1) (a) Hoeben, F. J. M.; Jonkheijm, P.; Meijer, E. W.; Schenning, A. P. H. J. *Chem. Rev.* **2005**, *105*, 1491–1546. (b) Würthner, F., Ed. Supramolecular Dye Chemistry. In *Topics in Current Chemistry*; Springer-Verlag: Berlin, 2005; p 258. (c) Wu, J.; Pisula, W.; Müllen, K. *Chem. Rev.* **2007**, *107*, 718–747. (d) Grimsdale, A. C.; Müllen, K. *Angew. Chem., Int. Ed.* **2005**, *44*, 5592–5629. (e) Schenning, A. P. H. J.; Meijer, E. W. *Chem. Commun.* **2005**, 3245–3258. (f) Zang, L.; Che, Y.; Moore, J. S. *Acc. Chem. Res.* **2008**, *41*, 1596–1608. (g) Babu, S. S.; Prasanthkumar, S.; Ajayaghosh, A. *Angew. Chem., Int. Ed.* **2012**, *51*, 1766–1776.

(2) (a) Würthner, F. *Chem. Commun.* **2004**, 1564–1579. (b) Langhals, H. *Heterocycles* **1995**, *40*, 477–500. (c) Wasielewski, M. R. *Acc. Chem. Res.* **2009**, *42*, 1910–1921. (d) Zhan, X.; Facchetti, A.; Barlow, S.; Marks, T. J.; Ratner, M. A.; Wasielewski, M. R.; Marder, S. R. *Adv. Mater.* **2011**, *23*, 268–284. (e) Herrmann, A.; Müllen, K. *Chem. Lett.* **2006**, *35*, 978–985.

(3) Elemans, J. A. A. W.; van Hameren, R.; Nolte, R. J. M.; Rowan, A. E. *Adv. Mater.* **2006**, *18*, 1251–1266.

(4) Horowitz, G.; Kouki, F.; Spearman, P.; Fichou, D.; Nogues, C.; Pan, X.; Garnier, F. *Adv. Mater.* **1996**, *8*, 242–245.

(5) (a) Graser, F.; Haedicke, E. *Liebigs Ann. Chem.* **1980**, 1994–2011. (b) Klebe, G.; Graser, F.; Hadicke, E.; Berndt, J. *Acta Crystallogr., Sect. B: Struct. Crystallogr. Cryst. Chem.* **1989**, *45*, 69–77. (c) Mizuguchi, J.; Tojo, K. *J. Phys. Chem. B* **2002**, *106*, 767–772. (d) Wang, W.; Han, J. J.; Wang, L.-Q.; Li, L.-S.; Shaw, W. J.; Li, A. D. Q. *Nano Lett.* **2003**, *3*, 455–458.

(6) (a) Li, C.; Wonneberger, H. *Adv. Mater.* **2012**, *24*, 613–636. (b) Nagao, Y. *Prog. Org. Coat.* **1997**, *31*, 43–49.

(7) Würthner, F.; Thalacker, C.; Diele, S.; Tschierske, C. *Chem.—Eur. J.* **2001**, *7*, 2245–2253.

(8) (a) Rosen, B. M.; Wilson, C. J.; Wilson, D. A.; Peterca, M.; Imam, M. R.; Percec, V. *Chem. Rev.* **2009**, *109*, 6275–6540. (b) Babu, S. S.; Mohwald, H.; Nakanishi, T. *Chem. Soc. Rev.* **2010**, *39*, 4021–4035.

(9) Dehm, V.; Chen, Z.; Baumeister, U.; Prins, P.; Siebbeles Laurens, D. A.; Würthner, F. *Org. Lett.* **2007**, *9*, 1085–1088.

(10) (a) Chen, Z.; Stepanenko, V.; Dehm, V.; Prins, P.; Siebbeles, L. D. A.; Seibt, J.; Marquetand, P.; Engel, V.; Würthner, F. *Chem.—Eur. J.* **2007**, *13*, 436–449. (b) Percec, V.; Peterca, M.; Tadjiev, T.; Zeng, X.; Ungar, G.; Leowanawat, P.; Aqad, E.; Imam, M. R.; Rosen, B. M.; Akbey, U.; Graf, R.; Sekharan, S.; Sebastiani, D.; Spiess, H. W.; Heiney, P. A.; Hudson, S. D. *J. Am. Chem. Soc.* **2011**, *133*, 12197–12219. (c) Percec, V.; Aqad, E.; Peterca, M.; Imam, M. R.; Glodde, M.; Bera, T. K.; Miura, Y.; Balagurusamy, V. S. K.; Ewbank, P. C.; Würthner, F.; Heiney, P. A. *Chem.—Eur. J.* **2007**, *13*, 3330–3345. (d) An, Z.; Yu, J.; Jones, S. C.; Barlow, S.; Yoo, S.; Domercq, B.; Prins, P.; Siebbeles, L. D. A.; Kippelen, B.; Marder, S. R. *Adv. Mater.* **2005**, *17*, 2580–2583. (e) Kato, T.; Mizoshita, N.; Kishimoto, K. *Angew. Chem., Int. Ed.* **2006**, *45*, 38–68.

(11) Marcon, V.; Breiby, D. W.; Pisula, W.; Dahl, J.; Kirkpatrick, J.; Patwardhan, S.; Grozema, F.; Andrienko, D. *J. Am. Chem. Soc.* **2009**, *131*, 11426–11432.

(12) (a) Fuller, M. J.; Sinks, L. E.; Rybtchinski, B.; Giaimo, J. M.; Li, X.; Wasielewski, M. R. *J. Phys. Chem. A* **2005**, *109*, 970–975. (b) Schmidt-Mende, L.; Fechtenkotter, A.; Müllen, K.; Moons, E.; Friend, R. H.; MacKenzie, J. D. *Science* **2001**, *293*, 1119–1122. (c) Balakrishnan, K.; Datar, A.; Naddo, T.; Huang, J.; Oitker, R.; Yen, M.; Zhao, J.; Zang, L. *J. Am. Chem. Soc.* **2006**, *128*, 7390–7398. (d) Wicklein, A.; Lang, A.; Muth, M.; Thelakkat, M. *J. Am. Chem. Soc.* **2009**, *131*, 14442–14453. (e) Hansen, M. R.; Schnitzler, T.; Pisula, W.; Graf, R.; Müllen, K.; Spiess, H. W. *Angew. Chem., Int. Ed.* **2009**, *48*,

4621−4624. (f) Marcon, V.; Kirkpatrick, J.; Pisula, W.; Andrienko, D. *Phys. Status Solidi B* **2008**, *245*, 820−824. (g) Nolde, F.; Pisula, W.; Muller, S.; Kohl, C.; Müllen, K. *Chem. Mater.* **2006**, *18*, 3715−3725. (h) Cormier, R. A.; Gregg, B. A. *J. Phys. Chem. B* **1997**, *101*, 11004−11006. (i) Pisula, W.; Kastler, M.; Wasserfallen, D.; Robertson, J. W. F.; Nolde, F.; Kohl, C.; Müllen, K. *Angew. Chem., Int. Ed.* **2006**, *45*, 819−823.

(13) (a) Che, Y.; Datar, A.; Balakrishnan, K.; Zang, L. *J. Am. Chem. Soc.* **2007**, *129*, 7234−7235. (b) Che, Y.; Datar, A.; Yang, X.; Naddo, T.; Zhao, J.; Zang, L. *J. Am. Chem. Soc.* **2007**, *129*, 6354−6355.

(14) (a) Schwartz, E.; Le Gac, S.; Cornelissen, J. J. L. M.; Nolte, R. J. M.; Rowan, A. E. *Chem. Soc. Rev.* **2010**, *39*, 1576−1599. (b) De Witte, P. A. J.; Hernando, J.; Neuteboom, E. E.; van Dijk, E. M. H. P.; Meskers, S. C. J.; Janssen, R. A. J.; van Hulst, N. F.; Nolte, R. J. M.; Garcia-Parajo, M. F.; Rowan, A. E. *J. Phys. Chem. B* **2006**, *110*, 7803−7812. (c) Dehm, V.; Buchner, M.; Seibt, J.; Engel, V.; Würthner, F. *Chem. Sci.* **2011**, *2*, 2094−2100. (d) Sommer, M.; Lang, A. S.; Thelakkat, M. *Angew. Chem., Int. Ed.* **2008**, *47*, 7901−7904. (e) Schwartz, E.; Palermo, V.; Finlayson, C. E.; Huang, Y.-S.; Otten, M. B. J.; Liscio, A.; Trapani, S.; González-Valls, I.; Brocorens, P.; Cornelissen, J. J. L. M.; Peneva, K.; Müllen, K.; Spano, F. C.; Yartsev, A.; Westenhoff, S.; Friend, R. H.; Beljonne, D.; Nolte, R. J. M.; Samorì, P.; Rowan, A. E. *Chem.—Eur. J.* **2009**, *15*, 2536−2547. (f) Hernando, J.; de Witte, P. A. J.; van Dijk, E. M. H. P.; Korterik, J.; Nolte, R. J. M.; Rowan, A. E.; García-Parajó, M. F.; van Hulst, N. F. *Angew. Chem., Int. Ed.* **2004**, *43*, 4045−4049. (g) Palermo, V.; Schwartz, E.; Finlayson, C. E.; Liscio, A.; Otten, M. B. J.; Trapani, S.; Müllen, K.; Beljonne, D.; Friend, R. H.; Nolte, R. J. M.; Rowan, A. E.; Samorì, P. *Adv. Mater.* **2009**, *22*, E81−E88. (h) Dabirian, R.; Palermo, V.; Liscio, A.; Schwartz, E.; Otten, M. B. J.; Finlayson, C. E.; Treossi, E.; Friend, R. H.; Calestani, G.; Müllen, K.; Nolte, R. J. M.; Rowan, A. E.; Samori, P. *J. Am. Chem. Soc.* **2009**, *131*, 7055−7063. (i) Neuteboom, E. E.; van Hal, P. A.; Janssen, R. A. J. *Chem.—Eur. J.* **2004**, *10*, 3907−3918. (j) Neuteboom, E. E.; Meskers, S. C. J.; Meijer, E. W.; Janssen, R. A. J. *Macromol. Chem. Phys.* **2004**, *205*, 217−222.

(15) (a) Sugiyasu, K.; Fujita, N.; Shinkai, S. *Angew. Chem., Int. Ed.* **2004**, *43*, 1229−1233. (b) Li, X.-Q.; Stepanenko, V.; Chen, Z.; Prins, P.; Siebbeles Laurens, D. A.; Würthner, F. *Chem. Commun.* **2006**, 3871−3873. (c) Würthner, F.; Bauer, C.; Stepanenko, V.; Yagai, S. *Adv. Mater.* **2008**, *20*, 1695−1698. (d) Würthner, F.; Hanke, B.; Lysetska, M.; Lambright, G.; Harms, G. S. *Org. Lett.* **2005**, *7*, 967−970.

(16) (a) Whitesides, G. M.; Simanek, E. E.; Mathias, J. P.; Seto, C. T.; Chin, D.; Mammen, M.; Gordon, D. M. *Acc. Chem. Res.* **1995**, *28*, 37−44. (b) Lehn, J.-M. *Supramolecular Chemistry: Concepts and Perspectives*; VCH: Weinheim, 1995. (c) Prins, L. J.; Reinhoudt, D. N.; Timmerman, P. *Angew. Chem., Int. Ed.* **2001**, *40*, 2382−2426. (d) Zimmerman, S. C.; Corbin, P. S. *Struct. Bonding (Berlin)* **2000**, *96*, 63−94. (e) ten Cate, A. T.; Sijbesma, R. P. *Macromol. Rapid Commun.* **2002**, *23*, 1094−1112. (f) Sijbesma, R. P.; Meijer, E. W. *Chem. Commun.* **2003**, 5−16. (g) Sherrington, D. C.; Taskinen, K. A. *Chem. Soc. Rev.* **2001**, *30*, 83−93. (h) Yagai, S. *J. Photochem. Photobiol., C* **2006**, *7*, 164−182. (i) Gonzalez-Rodriguez, D.; Schenning, A. P. H. J. *Chem. Mater.* **2011**, *23*, 310−325. (j) Lena, S.; Masiero, S.; Pieraccini, S.; Spada, G. P. *Chem.—Eur. J.* **2009**, *15*, 7792−7806. (k) Kato, T. *Science* **2002**, *295*, 2414−2418. (l) Davis, J. T. *Angew. Chem., Int. Ed.* **2004**, *43*, 668−698.

(17) (a) Kimizuka, N.; Kawasaki, T.; Hirata, K.; Kunitake, T. *J. Am. Chem. Soc.* **1998**, *120*, 4094−4104. (b) Würthner, F.; Thalacker, C.; Sautter, A.; Schartl, W.; Ibach, W.; Hollricher, O. *Chem.—Eur. J.* **2000**, *6*, 3871−3886. (c) Schenning, A. P. H. J.; Jonkheijm, P.; Peeters, E.; Meijer, E. W. *J. Am. Chem. Soc.* **2001**, *123*, 409−416. (d) Kimizuka, N.; Kawasaki, T.; Hirata, K.; Kunitake, T. *J. Am. Chem. Soc.* **1995**, *117*, 6360−6361. (e) Würthner, F.; Thalacker, C.; Sautter, A. *Adv. Mater.* **1999**, *11*, 754−758. (f) Thalacker, C.; Würthner, F. *Adv. Funct. Mater.* **2002**, *12*, 209−218. (g) Schenning, A. P. H. J.; van Herrikhuyzen, J.; Jonkheijm, P.; Chen, Z.; Würthner, F.; Meijer, E. W. *J. Am. Chem. Soc.* **2002**, *124*, 10252−10253.

(18) (a) Sinks, L. E.; Rybtchinski, B.; Iimura, M.; Jones, B. A.; Goshe, A. J.; Zuo, X.; Tiede, D. M.; Li, X.; Wasielewski, M. R. *Chem. Mater.* **2005**, *17*, 6295−6303. (b) Würthner, F.; Chen, Z.; Hoeben, F. J. M.; Osswald, P.; You, C.-C.; Jonkheijm, P.; Herrikhuyzen, J. V.; Schenning, A. P. H. J.; van der Schoot, P. P. A. M.; Meijer, E. W.; Beckers, E. H. A.; Meskers, S. C. J.; Janssen, R. A. J. *J. Am. Chem. Soc.* **2004**, *126*, 10611−10618. (c) Yagai, S.; Monma, Y.; Kawauchi, N.; Karatsu, T.; Kitamura, A. *Org. Lett.* **2007**, *9*, 1137−1140. (d) Seki, T.; Yagai, S.; Karatsu, T.; Kitamura, A. *J. Org. Chem.* **2008**, *73*, 3328−3335. (e) Yagai, S.; Seki, T.; Murayama, H.; Wakikawa, Y.; Ikoma, T.; Kikkawa, Y.; Karatsu, T.; Kitamura, A.; Honsho, Y.; Seki, S. *Small* **2010**, *6*, 2731−2740.

(19) (a) Mathias, J. P.; Simanek, E. E.; Whitesides, G. M. *J. Am. Chem. Soc.* **1994**, *116*, 4326−4340. (b) Mathias, J. P.; Seto, C. T.; Simanek, E. E.; Whitesides, G. M. *J. Am. Chem. Soc.* **1994**, *116*, 1725−1736. (c) Mathias, J. P.; Simanek, E. E.; Zerkowski, J. A.; Seto, C. T.; Whitesides, G. M. *J. Am. Chem. Soc.* **1994**, *116*, 4316−4325.

(20) (a) Timmerman, P.; Vreekamp, R. H.; Hulst, R.; Verboom, W.; Reinhoudt, D. N.; Rissanen, K.; Udachin, K. A.; Ripmeester, J. *Chem.—Eur. J.* **1997**, *3*, 1823−1832. (b) Timmerman, P.; Jolliffe, K. A.; Calama, M. C.; Weidmann, J.-L.; Prins, L. J.; Cardullo, F.; Snellink-Ruel, B. H. M.; Fokkens, R. H.; Nibbering, N. M. M.; Shinkai, S.; Reinhoudt, D. N. *Chem.—Eur. J.* **2000**, *6*, 4104−4115. (c) Prins, L. J.; Thalacker, C.; Wurthner, F.; Timmerman, P.; Reinhoudt, D. N. *Proc. Natl. Acad. Sci. U.S.A.* **2001**, *98*, 10042−10045. (d) Prins, L. J.; Huskens, J.; De Jong, F.; Timmerman, P.; Reinhoudt, D. N. *Nature* **1999**, *398*, 498−502.

(21) Zerkowski, J. A.; Seto, C. T.; Whitesides, G. M. *J. Am. Chem. Soc.* **1992**, *114*, 5473−5475.

(22) Bielejewska, A. G.; Marjo, C. E.; Prins, L. J.; Timmerman, P.; de Jong, F.; Reinhoudt, D. N. *J. Am. Chem. Soc.* **2001**, *123*, 7518−753.

(23) (a) Choi, I. S.; Li, X.; Simanek, E. E.; Akaba, R.; Whitesides, G. M. *Chem. Mater.* **1999**, *11*, 684−690. (b) Yang, W.; Chai, X.; Chi, L.; Liu, X.; Cao, Y.; Lu, R.; Jiang, Y.; Tang, X.; Fuchs, H.; Li, T. *Chem.—Eur. J.* **1999**, *5*, 1144−1149. (c) Schonherr, H.; Paraschiv, V.; Zapotoczny, S.; Crego-Calama, M.; Timmerman, P.; Frank, C. W.; Vancso, G. J.; Reinhoudt, D. N. *Proc. Natl. Acad. Sci. U.S.A.* **2002**, *99*, 5024−5027. (d) Piermattei, A.; Giesbers, M.; Marcelis, A. T. M.; Mendes, E.; Picken, S. J.; Crego-Calama, M.; Reinhoudt, D. N. *Angew. Chem., Int. Ed.* **2006**, *45*, 7543−7546. (e) Yagai, S.; Nakajima, T.; Kishikawa, K.; Kohmoto, S.; Karatsu, T.; Kitamura, A. *J. Am. Chem. Soc.* **2005**, *127*, 11134−11139.

(24) (a) Huang, C.-H.; McClenaghan, N. D.; Kuhn, A.; Hofstraat, J. W.; Bassani, D. M. *Org. Lett.* **2005**, *7*, 3409−3412. (b) Yagai, S.; Mahesh, S.; Kikkawa, Y.; Unoike, K.; Karatsu, T.; Kitamura, A.; Ajayaghosh, A. *Angew. Chem., Int. Ed.* **2008**, *47*, 4691−4694. (c) Yagai, S.; Kubota, S.; Unoike, K.; Karatsu, T.; Kitamura, A. *Chem. Commun.* **2008**, 4466−4468. (d) Yagai, S.; Aonuma, H.; Kikkawa, Y.; Kubota, S.; Karatsu, T.; Kitamura, A.; Mahesh, S.; Ajayaghosh, A. *Chem.—Eur. J.* **2010**, *16*, 8652−8661. (e) Seki, T.; Asano, A.; Seki, S.; Kikkawa, Y.; Murayama, H.; Karatsu, T.; Kitamura, A.; Yagai, S. *Chem.—Eur. J.* **2011**, *17*, 3598−3608.

(25) (a) Jonkheijm, P.; Miura, A.; Zdanowska, M.; Hoeben, F. J. M.; De Feyter, S.; Schenning, A. P. H. J.; De Schryver, F. C.; Meijer, E. W. *Angew. Chem., Int. Ed.* **2004**, *43*, 74−78. (b) Borzsonyi, G.; Beingessner, R. L.; Yamazaki, T.; Cho, J.-Y.; Myles, A. J.; Malac, M.; Egerton, R.; Kawasaki, M.; Ishizuka, K.; Kovalenko, A.; Fenniri, H. *J. Am. Chem. Soc.* **2010**, *132*, 15136−15139. (c) Barbera, J.; Puig, L.; Romero, P.; Serrano, J. L.; Sierra, T. *J. Am. Chem. Soc.* **2005**, *127*, 458−464. (d) Yagai, S.; Kinoshita, T.; Kikkawa, Y.; Karatsu, T.; Kitamura, A.; Honsho, Y.; Seki, S. *Chem.—Eur. J.* **2009**, *15*, 9320−9324. (e) Yagai, S.; Kubota, S.; Saito, H.; Unoike, K.; Karatsu, T.; Kitamura, A.; Ajayaghosh, A.; Kanesato, M.; Kikkawa, Y. *J. Am. Chem. Soc.* **2009**, *131*, 5408−5410. (f) Yagai, S.; Goto, Y.; Karatsu, T.; Kitamura, A.; Kikkawa, Y. *Chem.—Eur. J.* **2011**, *17*, 13657−13660.

(26) Yagai, S.; Karatsu, T.; Kitamura, A. *Chem. Commun.* **2003**, 1844−1845.

(27) van Herrikhuyzen, J.; Syamakumari, A.; Schenning, A. P. H. J.; Meijer, E. W. *J. Am. Chem. Soc.* **2004**, *126*, 10021−10027.

(28) Ghosh, S.; Li, X.-Q.; Stepanenko, V.; Würthner, F. *Chem.—Eur. J.* **2008**, *14*, 11343−11357.

(29) (a) Yagai, S.; Seki, T.; Karatsu, T.; Kitamura, A.; Würthner, F. *Angew. Chem., Int. Ed.* **2008**, *47*, 3367−3371. (b) Struijk, C. W.; Sieval, A. B.; Dakhorst, J. E. J.; van Dijk, M.; Kimkes, P.; Koehorst, R. B. M.; Donker, H.; Schaafsma, T. J.; Picken, S. J.; van de Craats, A. M.; Warman, J. M.; Zuilhof, H.; Sudholter, E. J. R. *J. Am. Chem. Soc.* **2000**, *122*, 11057−11066. (c) Gregg, B. A. *J. Phys. Chem.* **1996**, *100*, 852−859.
(30) Martin, R. B. *Chem. Rev.* **1996**, *96*, 3043−3064.
(31) Zhao, D.; Moore, J. S. *Org. Biomol. Chem.* **2003**, *1*, 3471−3491.
(32) (a) Simic, V.; Bouteiller, L.; Jalabert, M. *J. Am. Chem. Soc.* **2003**, *125*, 13148−13154. (b) Jadzyn, J.; Stockhausen, M.; Zywucki, B. *J. Phys. Chem.* **1987**, *91*, 754−757. (c) Percec, V.; Ungar, G.; Peterca, M. *Science* **2006**, *313*, 55−56. (d) Jonkheijm, P.; van der Schoot, P.; Schenning, A. P. H. J.; Meijer, E. W. *Science* **2006**, *313*, 80−83. (e) Smulders, M. M. J.; Schenning, A. P. H. J.; Meijer, E. W. *J. Am. Chem. Soc.* **2007**, *130*, 606−611. (f) Smulders, M. M. J.; Nieuwenhuizen, M. M. L.; Greef, T. F. A. d.; van-der-Schoot, P.; Schenning, A. P. H. J.; Meijer, E. W. *Chem.—Eur. J.* **2010**, *16*, 362−367.
(33) Arnaud, A.; Belleney, J.; Boué, F.; Bouteiller, L.; Carrot, G.; Wintgens, V. *Angew. Chem., Int. Ed.* **2004**, *43*, 1718−1721.
(34) Kaiser, T. E.; Stepanenko, V.; Würthner, F. *J. Am. Chem. Soc.* **2009**, *131*, 6719−6732.
(35) Chen, Z.; Lohr, A.; Saha-Moller, C. R.; Würthner, F. *Chem. Soc. Rev.* **2009**, *38*, 564−584.
(36) Iverson, I. K.; Tam-Chang, S.-W. *J. Am. Chem. Soc.* **1999**, *121*, 5801−5802.
(37) von Berlepsch, H.; Boettcher, C.; Daehne, L. *J. Phys. Chem. B* **2000**, *104*, 8792−8799.
(38) (a) Würthner, F.; Yao, S.; Beginn, U. *Angew. Chem., Int. Ed.* **2003**, *42*, 3247−3250. (b) Yao, S.; Beginn, U.; Gress, T.; Lysetska, M.; Würthner, F. *J. Am. Chem. Soc.* **2004**, *126*, 8336−8348. (c) Yagai, S.; Kinoshita, T.; Higashi, M.; Kishikawa, K.; Nakanishi, T.; Karatsu, T.; Kitamura, A. *J. Am. Chem. Soc.* **2007**, *129*, 13277−13287.
(39) (a) Fouquey, C.; Lehn, J. M.; Levelut, A. M. *Adv. Mater.* **1990**, *2*, 254−257. (b) Giorgi, T.; Lena, S.; Mariani, P.; Cremonini, M. A.; Masiero, S.; Pieraccini, S.; Rabe, J. P.; Samori, P.; Spada, G. P.; Gottarelli, G. *J. Am. Chem. Soc.* **2003**, *125*, 14741−14749.
(40) Percec, V.; Aqad, E.; Peterca, M.; Imam, M. R.; Glodde, M.; Bera, T. K.; Miura, Y.; Balagurusamy, V. S. K.; Ewbank, P. C.; Würthner, F.; Heiney, P. A. *Chem.—Eur. J.* **2007**, *13*, 3330−3345.
(41) Yagai, S.; Nakano, Y.; Seki, S.; Asano, A.; Okubo, T.; Isoshima, T.; Karatsu, T.; Kitamura, A.; Kikkawa, Y. *Angew. Chem., Int. Ed.* **2010**, *49*, 9990−9994.
(42) Shaller, A. D.; Wang, W.; Li, A.; Moyna, G.; Han, J. J.; Helms, G. L.; Li, A. D. Q. *Chem.—Eur. J.* **2011**, *17*, 8350−8362.
(43) Hansen, M. R.; Graf, R.; Sekharan, S.; Sebastiani, D. *J. Am. Chem. Soc.* **2009**, *131*, 5251−5256.
(44) Seki, T.; Maruya, Y.; Nakayama, K.-i.; Karatsu, T.; Kitamura, A.; Yagai, S. *Chem. Commun.* **2011**, *47*, 12447−12449.
(45) Fenniri, H.; Mathivanan, P.; Vidale, K. L.; Sherman, D. M.; Hallenga, K.; Wood, K. V.; Stowell, J. G. *J. Am. Chem. Soc.* **2001**, *123*, 3854−3855.
(46) Whitesides, G. M.; Mathias, J. P.; Seto, C. T. *Science* **1991**, *254*, 1312−1319.
(47) (a) Zerkowski, J. A.; Seto, C. T.; Wierda, D. A.; Whitesides, G. M. *J. Am. Chem. Soc.* **1990**, *112*, 9025−9026. (b) Zerkowski, J. A.; MacDonald, J. C.; Seto, C. T.; Wierda, D. A.; Whitesides, G. M. *J. Am. Chem. Soc.* **1994**, *116*, 2382−2391. (c) Zerkowski, J. A.; Mathias, J. P.; Whitesides, G. M. *J. Am. Chem. Soc.* **1994**, *116*, 4305−4315. (d) Zerkowski, J. A.; MacDonald, J. C.; Whitesides, G. M. *Chem. Mater.* **1994**, *6*, 1250−1257. (e) Zerkowski, J. A.; Whitesides, G. M. *J. Am. Chem. Soc.* **1994**, *116*, 4298−4304.
(48) (a) Plasseraud, L.; Cuervo, L. G.; Guillon, D.; Suess-Fink, G.; Deschenaux, R.; Bruce, D. W.; Donnio, B. *J. Mater. Chem.* **2002**, *12*, 2653−2658. (b) Yagai, S.; Kubota, S.; Iwashima, T.; Kishikawa, K.; Nakanishi, T.; Karatsu, T.; Kitamura, A. *Chem.—Eur. J.* **2008**, *14*, 5246−5257. (c) Würthner, F.; Yao, S.; Heise, B.; Tschierske, C. *Chem. Commun.* **2001**, 2260−2261. (d) Yagai, S.; Iwashima, T.; Kishikawa, K.; Nakahara, S.; Karatsu, T.; Kitamura, A. *Chem.—Eur. J.* **2006**, *12*, 3984−3994. (e) Kohlmeier, A.; Janietz, D. *Chem.—Eur. J.* **2010**, *16*, 10453−10461.
(49) (a) Koyano, H.; Bissel, P.; Yoshihara, K.; Ariga, K.; Kumitake, T. *Chem.—Eur. J.* **1997**, *3*, 1077−1082. (b) Mascal, M.; Hansen, J.; Fallon, P. S.; Blake, A. J.; Heywood, B. R.; Moore, M. H.; Turkenburg, J. P. *Chem.—Eur. J.* **1999**, *5*, 381−384.
(50) (a) Kimizuka, N.; Kawasaki, T.; Kunitake, T. *J. Am. Chem. Soc.* **1993**, *115*, 4387−4388. (b) Hanabusa, K.; Miki, T.; Taguchi, Y.; Koyama, T.; Shirai, H. *J. Chem. Soc., Chem. Commun.* **1993**, 1382−1384. (c) Kanie, K.; Yasuda, T.; Kato, T.; Ujiie, S. *Chem. Commun.* **2000**, 1899−1900. (d) Kanie, K.; Nishii, M.; Yasuda, T.; Taki, T.; Ujiie, S.; Kato, T. *J. Mater. Chem.* **2001**, *11*, 2875−2886. (e) Seki, T.; Maruya, Y.; Nakayama, K.-i.; Karatsu, T.; Kitamura, A.; Yagai, S. *Chem. Commun.* **2011**, *47*, 12447−12449.
(51) (a) Araki, K.; Takasawa, R.; Yoshikawa, I. *Chem. Commun.* **2001**, 1826−1827. (b) Sessler, J. L.; Sathiosatham, M.; Doerr, K.; Lynch, V.; Abboud, K. A. *Angew. Chem., Int. Ed.* **2000**, *39*, 1300−1303. (c) Cai, M.; Shi, X.; Sidorov, V.; Fabris, D.; Lam, Y.-f.; Davis, J. T. *Tetrahedron* **2002**, *58*, 661−671. (d) Giorgi, T.; Grepioni, F.; Manet, I.; Mariani, P.; Masiero, S.; Mezzina, E.; Pieraccini, S.; Saturni, L.; Spada, G. P.; Gottarelli, G. *Chem.—Eur. J.* **2002**, *8*, 2143−2152. (e) Gottarelli, G.; Masiero, S.; Mezzina, E.; Pieraccini, S.; Rabe, J. P.; Samori, P.; Spada, G. P. *Chem.—Eur. J.* **2000**, *6*, 3242−3248. (f) Mezzina, E.; Mariani, P.; Itri, R.; Masiero, S.; Pieraccini, S.; Spada, G. P.; Spinozzi, F.; Davis, J. T.; Gottarelli, G. *Chem.—Eur. J.* **2001**, *7*, 388−395. (g) Ciesielski, A.; Lena, S.; Masiero, S.; Spada, G. P.; Samorì, P. *Angew. Chem., Int. Ed.* **2010**, *49*, 1963−1966.
(52) Kato, T.; Matsuoka, T.; Nishii, M.; Kamikawa, Y.; Kanie, K.; Nishimura, T.; Yashima, E.; Ujiie, S. *Angew. Chem., Int. Ed.* **2004**, *43*, 1969−1972.
(53) Mizuguchi, J. *J. Appl. Phys.* **1998**, *84*, 4479−4486.
(54) (a) Warman, J. M.; de Haas, M. P.; Dicker, G.; Grozema, F. C.; Piris, J.; Debije, M. G. *Chem. Mater.* **2004**, *16*, 4600−4609. (b) Saeki, A.; Seki, S.; Koizumi, Y.; Sunagawa, T.; Ushida, K.; Tagawa, S. *J. Phys. Chem. B* **2005**, *109*, 10015−10019.
(55) (a) Ford, W. E.; Hiratsuka, H.; Kamat, P. V. *J. Phys. Chem.* **1989**, *93*, 6692−6696. (b) Gosztola, D.; Niemczyk, M. P.; Svec, W.; Lukas, A. S.; Wasielewski, M. R. *J. Phys. Chem. A* **2000**, *104*, 6545−6551.
(56) (a) Tauber, M. J.; Kelley, R. F.; Giaimo, J. M.; Rybtchinski, B.; Wasielewski, M. R. *J. Am. Chem. Soc.* **2006**, *128*, 1782−1783. (b) Hoogenboom, J. P.; van Dijk, E. M. H. P.; Hernando, J.; van Hulst, N. F.; Garcia-Parajo, M. F. *Phys. Rev. Lett.* **2005**, *95*, 097401. (c) Gronheid, R.; Stefan, A.; Cotlet, M.; Hofkens, J.; Qu, J.; Müllen, K.; Van der Auweraer, M.; Verhoeven, J. W.; De Schryver, F. C. *Angew. Chem., Int. Ed.* **2003**, *42*, 4209−4214. (d) Liu, R.; Holman, M. W.; Zang, L.; Adams, D. M. *J. Phys. Chem. A* **2003**, *107*, 6522−6526.
(57) Vysotsky, M. O.; Boehmer, V.; Würthner, F.; You, C.-C.; Rissanen, K. *Org. Lett.* **2002**, *4*, 2901−2904.
(58) (a) Ishi-i, T.; Shinkai, S. *Top. Curr. Chem.* **2005**, *258*, 119−160. (b) Yagai, S. In *Supramolecular Soft Matter*; Nakanishi, T., Ed.; Wiley-VCH: New York, 2011; pp 77−95.